Advances in Environmental Technology 11(2) 2025, 116-129.

Iranian Reasearch Organization for Science and Technology (IROST)

Advances in Environmental Technology

Journal home page: https://aet.irost.ir

Investigating microbial fuel cell performance by developing salt bridge from agar and activated carbon derived from pine cones

Anuj Saini*, Vijay Shankar

Department of Civil Engineering, NIT Hamirpur, H.P., P. O. Box: 177005, India.

ARTICLE INFO

Document Type:
Research Paper

Article history:
Received 23 July 2024
Received in revised form
27 November 2024
Accepted 3 December 2024

Keywords:
COD Removal
Current
Power Density
Voltage

ABSTRACT

The Microbial Fuel Cell (MFC) is a sustainable innovation that treats wastewater and yields energy by degrading organic matter. An agar salt bridge is an essential component of MFC, which reduces its cost and allows hydrogen ion transfer. This study focused on using activated carbon produced from pine cones (ACPC) in the preparation of the agar salt bridge. In the present study, the concentration of agar and ACPC was varied to develop different MFC setups designated as MFC-1, 2, and 3. The optimum dose of agar and ACPC was observed in MFC-1, which contained 2% (w/v) ACPC with 8% (w/v) agar. The maximum value of open circuit voltage, current, power density, and COD removal efficiency for MFC-1 was 421 mV, 1.052 A, 61.51 mW/m2, and 65.84%, respectively. Activated carbon has a high specific surface area, allowing for a higher number of proton transfers through the agar salt bridge. Because of the effective ion transfer in MFC-1, the voltage and current values increased until day four and remained stable until day twelve, beyond which the output decreased; however, the MFC-1 continued to provide readings up to the twentieth day of the investigations. The outcome of the study clearly indicates the potential of using ACPC in agar salt bridges to enhance the efficient transportation of hydrogen ions.

1. Introduction

Continuous use of non-renewable fuels has led to global warming, air pollution, and environmental degradation. Innovative approaches to power generation are necessary to transform the ambient energy sources into electrical energy [1-7]. Wastewater is increasingly being considered a useful commodity for energy and water conservation [8-9]. A sustainable approach is required to utilize wastewater in a way that ensures clean water and energy [10]. One such appealing technology is the Microbial Fuel Cell (MFC), which provides an alternate solution for treating wastewater and generating energy, achieving more than 50% COD reduction [11-12]. In the present study, dual chamber MFC was employed. It has three important parts: the anode, cathode, and salt bridge/Proton Exchange Membrane (PEM) [13]. Electrons are generated at the anode and migrate to the cathode via an external copper wire, while hydrogen ions (protons) move through the salt bridge to the cathode [14-15]. The protons (H+

*Corresponding author Tel.: +91 8700911789
E-mail: sainianuj222@gmail.com
DOI: 10.22104/AET.2024.7008.1923

ions) combine with electrons and oxygen (O2) in the aerobic conditions available in the cathode chamber of MFC [16]. To summarise, bacteria react with the solids present in the wastewater, biologically converting the wastewater into clean water, and electrons and H+ ions are produced during the process, which contributes to power generation [17]. Equations 1 and 2 explain the reactions occurring at the cathode and anode compartments, respectively [18-21]. Figure 1 depicts the dual-chambered MFC's schematic diagram.

$$4H^+ + 4e^- + O_2(Supplied\ externally) \rightarrow 4H_2O\ (aerobic\ conditions) \quad (1)$$

Anodic reaction:

$$Organic\ waste + microbes \rightarrow CO_2 + H^+ + e^-(anaerobic\ condition) \quad (2)$$

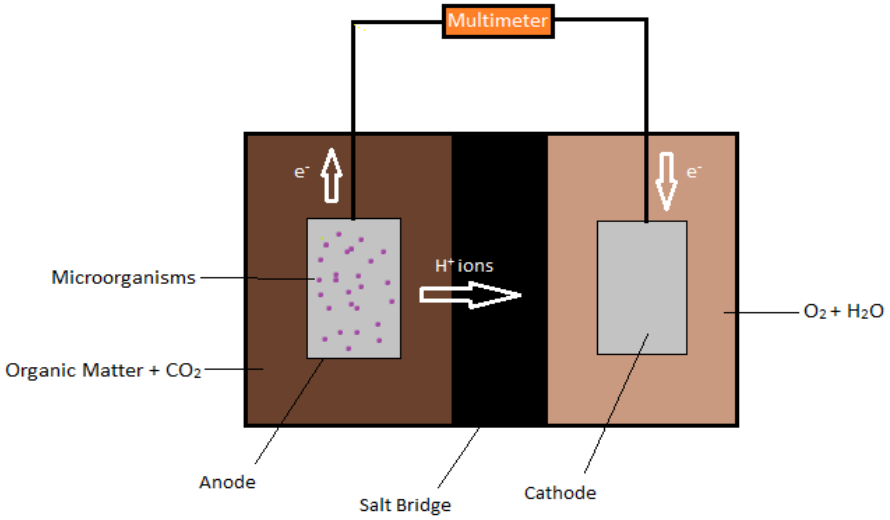

Fig. 1. Dual-chambered MFC schematic diagram.

According to [22], carbon-based materials are widely used as anode and cathode electrodes in MFCs because of their affordability and good efficiency. Graphite rods, which are inexpensive and readily available, are a good choice for electrode material and have been employed in the current study [23-24]. The salt bridge in MFCs, another major component affecting performance, structurally separates the two chambers and aids in transporting hydrogen ions to the cathode chamber. It also prevents oxygen from entering the anode chamber. Activated carbon (AC) is a valuable product utilized in MFCs to increase its efficiency [25].

Regarding emissions of acid and greenhouse gases, AC is more environmentally friendly than carbons derived from coal [26]. AC is utilized to improve electrode performance and to boost the electrochemical productivity of MFCs [27-28]. AC is inexpensive and possesses highly porous properties, ensuring a large specific surface area, which helps in high water retention, as confirmed by [29]. [16] conducted a study in which they prepared a salt bridge using natural clay and AC derived from coconuts. Similarly, [31-31] developed an AC-based hybrid PEM with high water retention capacity and high proton transfer efficiency. [32] also prepared a type of PEM that improved its proton transfer efficiency using AC produced from coconut shells. It was observed in the literature review that limited studies have been conducted where AC was used in the preparation of salt bridges. Investigations have been conducted to fill the research gap regarding the use of AC for an agar salt bridge. In the present study, the combination of activated carbon produced from ACPC with NaCl was used to prepare an agar salt bridge for a dual-chamber MFC, and the following objectives were achieved:

1) To evaluate the variation of Agar-Agar and activated carbon produced from pine cone on Microbial Fuel cell performance.

2) To assess the efficacy of different Microbial Fuel cell setups in measuring the daily current, open circuit voltage, power density, and coulombic efficiency values.

3) To conduct a comparative evaluation of different Microbial Fuel cell setups, based on COD removal efficiency at the beginning and end of the investigation.

2. Materials and methods

2.1. Apparatus and chemicals used

Materials and chemicals needed to prepare the MFC setups included Agar-Agar technical procured from Merck Life Science, India, and sodium chloride (assay 99.9%). Analytical-grade chemicals and reagents were utilized untreated. A variety of instruments and apparatus were used in this study: a COD digestor with a temperature range of 150oC by IKON instruments, India; a Bruaneur Emmett Teller (Quanta chrome Autosorb 1C BET Surface Area and Pore Volume Analyzer); a weighing balance with an accuracy of 0.001g by Danwer Scales, India; an oven; a muffle furnace (220-230V, 900oC by Instrument and Chemical pvt ltd, India); and a conical flask (500 ml) and a burette (50 ml) (Both by Borosil limited, India).

2.2. Preparation of lab-scale setups

The preparation of the salt bridge involved collecting pine cones from chir pine trees found in the western Himalayan region. These pine cones are natural waste products and can be used to create activated carbon, aiding in cleaning the environment. The pine cones were carbonised in a muffle furnace to create activated carbon, which was employed in preparing the salt bridge [33-34]. To utilise the property of the pine cones in producing activated carbon, a proximate analysis was performed to compute the percentage of volatile matter and moisture, fixed carbon available in organic material, and amount of ash. Pore information and the total surface area of ACPC were evaluated by a Pore Volume Analyzer and Quanta chrome Autosorb 1C BET Surface Area. The agar salt bridge was prepared using 3M sodium chloride (NaCl), ACPC, and Agar-Agar technical (Merck). The agar salt bridge is less expensive compared to commercially available proton exchange membranes such as Nafion [35]. The mixture was heated above 100 degrees in a beaker using a hot plate device and stirred continuously until a black, gel-like structure, a property of the agar, was observed [36]. The black, gel-like substance was poured into a 4 cm long 2.5 cm diameter PVC pipe, as depicted in Figure 2. PVC was chosen for its durability and heat resistance property up to a certain limit [37]. Three sets of lab-scale MFC setups were constructed with the ACPC and Agar variations. Plastic jars with a capacity of 500 ml each were used for the investigation. Care was taken to prevent water leakage from the anode and cathode chambers. Domestic wastewater was acquired from the NIT Hamirpur sewage treatment facility. The Grab sampling method was adopted, following IS 3025 (Part 1) for sampling and preservation for sample collection. Wastewater was poured into the anode chamber, maintaining an operational volume of 400 ml to avoid spills. The concentrations of ACPC and agar were varied, as given in Table 1. An aquarium pump (SOBO, SB-348A) was used to aerate the cathode while the anode remained anaerobic, with air controlled by a pressure device. The complete setup is described in Figure 3. A 0.75 mm2 electrical copper wire linked the anode and cathode externally. A 400-ohm resistance completed the circuit, using graphite rods in each compartment. Electrode spacing was kept at 10 cm centre-to-centre. A digital multi-meter (Model no: CHY DT9205A+, China-made) measured the current and open circuit values. Throughout the experiment, readings were recorded four times daily, and an average reading for each day was calculated to represent a singular value for analysis.

Fig. 2. Freshly prepared salt bridge.

Fig. 3. Lab scale Dual Chambered MFC Model.

Table 1. Variation of ACPC and Agar in MFC-1, MFC-2, and MFC-3

Setup	ACPC (w/v)	Agar-Agar (w/v)
MFC 1	2%	8%
MFC 2	4%	6%
MFC 3	6%	4%
MFC-A	0	8%

2.3 COD measurement

The amount of oxygen required to decompose the biodegradable and non-biodegradable organic matter in sewage is determined with the help of a chemical oxygen demand test. COD values were calculated by titrating the wastewater sample solution prepared with standard Ferrous Ammonium Sulphate (FAS) solution, following the standard procedure, as mentioned in IS 3025-58 (2006) [38].

2.4 Coulombic Efficiency (CE)

CE is the ratio of the total charge (in terms of coulombs) transported to the anode after bioelectro-oxidation of the substrate to the maximum charge available if the complete substrate can be converted to current theoretically. CE is calculated as per Equation 3 [39-41].

$$CE\ (\%) = \frac{M_{O_2} \int_0^{t_b} idt}{F * b * V_{an} * \Delta COD} * 100 \quad (3)$$

where M_(O_2) is the molecular oxygen weight of oxygen, 32 g/mol; F is Faraday's constant, C/mol; tb is the operation time of one MFC cycle, s; b is the number of electrons exchanged per mole of oxygen, 4 mol/e/ mol; and V is the volume of the anodic chamber, L.

3. Results and discussion

3.1 Proximate analysis and textural properties of ACPC

The results of the proximate analysis for ACPC shown in Table 2 indicate the percentage of fixed carbon is 22.56%, implying the significant capability for activated carbon preparation. The textural properties of ACPC are given in Table 3

3.2. Effects of variation of ACPC and Agar on cell performance

Three lab-scale models of different concentrations of activated carbon produced from ACPC and agar and one lab-scale model of MFC without the addition of ACPC were prepared, as shown in Table 1. All MFC setups showed a continuous increase in the open circuit voltage (OCV) values from day one to day four, as shown in Figure 4. The primary reason for the increase in OCV value was the degradation of organic matter in the sample and then the production of electrons and H+ ions in the anode chamber. Electrons were generated through the decomposition of organic matter and transferred through a direct electron transfer mechanism explained by [42]. For MFC-1 (2% ACPC and 8% agar), the value of OCV remained constant

until the twelfth day of the experiment and produced a maximum output of 421 mV; it was higher than that of the MFC-A (0% ACPC and 8% agar) output, i.e., 295mV, which did not employ ACPC. The maximum value of OCV produced by MFC-1 was also higher than the value recorded by [18]. Readings were recorded four times daily, and a daily average was calculated based on these four readings until the end of the experiment. MFC-1 provided readings until the 23rd day of the experiment, and the duration of giving continuous readings was higher than that recorded by [18], which was only eighteen days. The OCV values given in the last days of the investigation were quite low. This was due to the diminishing nature of the life cycle of the prepared agar salt bridge. The same trend was followed for MFC-2 (4% ACPC and 6% agar) as was observed in MFC-1. The maximum observed value corresponding to OCV in MFC-2 was 370 mV, which was higher than the value recorded by MFC-A. The possible explanation for this higher OCV value was due to less membrane resistance by using ACPC, which eased the transportation of a greater number of protons or hydrogen ions through the salt bridge. The AC's high specific surface area resulted in high absorptive capacity [16]. Hence, it was observed that the value of OCV was higher when ACPC was at 2% (w/v) compared to 4% and 6% in the salt bridge; this was attributed to the high absorptive capacity and superior specific surface area characteristics of AC that retained bound water and aided in increasing the proton conductivity across the anode to the cathode.

Even though the concentration of ACPC in both MFC-2 and MFC-3 was higher, the OCV values obtained were less than MFC-1. This was due to the decreasing agar content in both MFC-2 and MFC-3. The values of OCV started decreasing in each MFC setup within a span of 8-12 days. For MFC-1 and MFC-2, the OCV values started decreasing after twelve days, whereas for MFC-3, they decreased after the eighth day.

Table 2. Calculation for proximate analysis of ACPC.

Parameter	Weight (g)	Relation	Percentage (%)
Sample wt. (W_1)	10.65		
Moisture content sample dried at 105°C for 6 h (W_2)	8.93	$\frac{(W_1 - W_2)}{W_1} \times 100$	16.15
Volatile matter – sample W_2 dried at 700-950°C (W_3)	2.931	$\frac{(W_2 - W_3)}{W_1} \times 100$	56.33
Ash – combustion at 550°C for 1 h (W_4)	0.459	$\frac{W_4}{W_1} \times 100$	4.31
Fixed carbon		$100 - (W_2 + W_3 + W_4)$	23.21

Table 3. Textural properties of activated carbon produced from pine cones.

Material	Surface area (m^2/g)	Pore Size (nm)	Pore Volume (cm^3/g)
ACPC	194	8.32	5.6

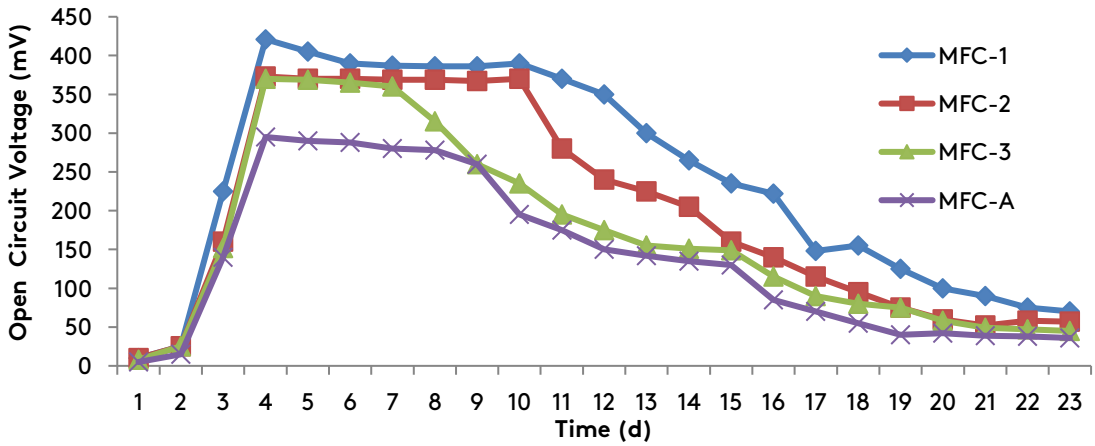

Fig. 4. Variation of open circuit voltage (mV) v/s time (days),

The maximum observed OCV value for MFC-3 was 341.05 mV. In MFC-3, OCV values started rising from day one to day four, remaining constant for only up to eight days; thus, a different trend was observed. A possible explanation for this trend would be the diminishing life cycle of the agar salt bridge. In this case, the salt bridge was organic in nature, and hence, its life span was liable to be reduced after 18-20 days. MFC-3 (6% ACPC and 4% agar) started to show a decline in OCV values beginning on the eighth day, which was clearly prior to that of MFC-1 and MFC-2. This was attributed to the lowest agar content (4%) in MFC-3, which was responsible for binding the contents of the salt bridge. There will be an ineffective transfer of hydrogen ions through the salt bridge with a low content of agar; hence, a sudden drop in the OCV value could be observed in MFC-3.

In MFC-1, the values of OCV remained constant for up to twelve days after peak OCV was achieved and then decreased gradually till the end-of-life span of the salt bridge; OCV values for MFC-3 remained constant for up to eight days only, and then there was a sharp drop in OCV values, as shown in Figure 4. Similarly, there was a sudden drop after the tenth day for MFC-2, and then OCV values decreased gradually. The explanation for this behavior is due to the decrease in proton conductivity due to low agar concentration in the salt bridge, which increased membrane resistance for proton transfer, as discussed by [43]. MFC-3 only contained 4% of agar, whereas MFC-1 contained 8% of agar. Hence, it is established that when agar content decreased, the attained peak value of OCV was low, as depicted in Figure 4. Every MFC setup with ACPC produced an output voltage higher than that of the MFC setup without ACPC addition, indicating that including ACPC improved the voltage output. Table 5 gives the peak values of open circuit voltage for each MFC setup. An investigation was also conducted for the efficacy of the agar salt bridge using concentrations of ACPC 1% (w/v) and 3% (w/v), but the results were not encouraging.

3.3. Current measurement in agar-based dual chamber MFC

The current was measured using a digital multimeter with a resistance of 400 ohms. The values were recorded four times daily, and a daily average was calculated based on these four readings until the end of the experiment. MFC-1 (2% ACPC and 8% agar) produced the highest peak current value of 1.052 mA, MFC-2 produced a current value of 0.951 mA, and MFC-3 gave the peak value of 0.938 mA, whereas MFC-A (0% ACPC and 8% agar) gave the lowest peak value of 0.737 mA. This is explained by Ohm's law Eq. 4, which rules that when resistance is kept constant, the value of the current is directly proportional to the voltage. Hence, it was observed that the plot of current values and time depicted in Figure 5 was almost similar to the plot of voltage and time shown in Figure 4.

$$V = I \times R \tag{4}$$

For MFC-1, the current value increased from day one to day four, which remained constant for up to twelve days. This could be important information needed to scale up the MFC for the pilot scale model. The same trend was followed by MFC-2, where the current value started rising from day one and continued until day four; then, the value remained constant for ten days. The current value for MFC-3 started rising from day one to day four, continued up to only eight days, and dropped suddenly. For MFC-1, the current started decreasing gradually after the twelfth day until the end of the life span of the salt bridge. Both MFC-2 and MFC-3 experienced a sudden drop in current values at ten and eight days of the investigation, respectively. This was due to the improper transfer of H+ ions and the decrease in the agar concentration in the MFC-3 (4% Agar) setup. On the twelfth day, current values for MFC-1, MFC-2, MFC-3, and MFC-A were 0.96 mA, 0.71 mA, 0.44 mA, and 0.35 mA, respectively. When ACPC was added to MFC-1, MFC-2, and MFC-3, it was found that the current values generated by these MFC setups were higher than those produced by MFC-A in which no ACPC was added. Also, the current values were higher than those recorded by [18]. The peak values of the current for each MFC setup are given in Table 5. According to [45], the type of microbial community present in the biofilm influences the current output in MFC, which can be enhanced by further investigating the biofilm formed at the anode.

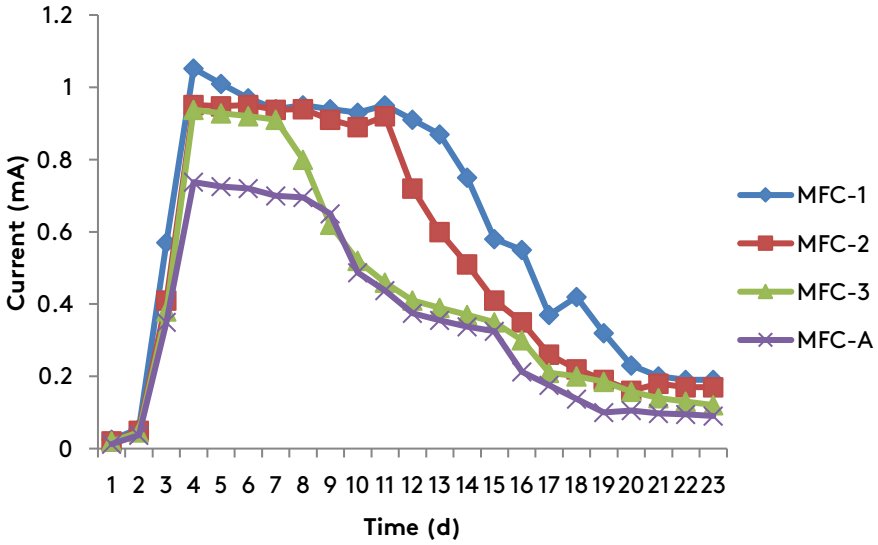

Fig. 5. Variation of current (mA) vs time (days) for MFC-1, MFC-2, and MFC-3.

3.4 COD removal efficiency

The COD was calculated using the Indian Standard Code IS 3025-58 (2006). Initial COD values were measured from the sample brought to the lab from the treatment plant under study. Then, the sample was transferred to the anode compartment of the MFC setup prepared in the laboratory named MFC-1, MFC-2, MFC-3, and MFC-A.

After the experiment, samples were taken out by opening the sealed anode compartment; then, the final COD values were calculated by following IS 3025-58 (2006). The formula used for COD calculation is given in Equation 5 (IS 3025-58).

$$COD = \frac{(V1-V2)\ N*8000}{Volume\ of\ sample\ taken\ in\ ml} \quad (5)$$

where V1 = volume of FAS required titration against the blank, in ml; V2 = volume of FAS required titration against the sample, in ml; and N = Normality of FAS.

Initial and final COD values were measured for each MFC setup and are given in Table 4. The initial value for the collected domestic wastewater sample was 490.5 mg/l. Final COD values for MFC-1, MFC-2, and MFC-3 were 167.55 mg/l, 199.34 mg/l, and 251.67 mg/l, respectively. It was observed that MFC-1 produced the lowest final COD values, which showed that MFC-1 achieved the highest treatment of wastewater with 2% ACPC and 8% agar. COD removal efficiency for MFC-1, MFC-2, MFC-3, and MFC-A was found to be 65.84%, 59.36%, 48.69%, and 46.82% respectively. This indicated that MFC-1 obtained the maximum COD removal efficiency. The COD removal efficiency in the present case exceeded the one reported by [18] for an MFC setup containing 10% (w/v) agar without using ACPC and an MFC-A setup investigated in the present study. The final COD removal efficiency achieved by [18] was 52.08%, which was less than the 65.84% obtained in the current study. The increased proton conductivity facilitated by using ACPC in the salt bridge helps retain bound water, which is essential for efficient H+ ions transfer across the agar salt bridge to the cathode chamber. This process helped maintain pH balance and increased microbial growth, ultimately contributing to higher COD removal efficiency. This correlation between H+ ions and high COD removal efficiency was illustrated by [16]. The COD values showed a reduction in all the MFC setups in the current study with time. The explanation for this behavior is the degradation of organic compounds by microorganisms available in wastewater. The whole process of decomposition reduced the COD of the wastewater, as confirmed by [18]. A comparison of the initial and final COD values can be observed in Figure 6. The maximum value of COD removal efficiency for each MFC setup is given in Table 4.

3.5 Coulombic Efficiency (CE)

According to Equation 3, the maximum coulombic efficiency of MFC-1, MFC-2, MFC-3, and MFC-A was 22.84%, 23.4%, 27.96%, and 19.98%, respectively. It

was observed that the operation of MFC in a fed-batch mode was advantageous in obtaining a high COD removal rate. Therefore, coulombic efficiencies obtained in these cases were low [45]. MFC-1 had the highest COD removal efficiency; hence, its CE was less compared to MFC-1 and MFC-2. The variation of CE with current density for MFC-1, MFC-2, MFC-3, and MFC-A is shown in Figure 7. It was observed that with the increase in current density, coulombic efficiency also rose. Also, the results showed that the MFC setups with ACPC addition in agar salt bridges had higher coulombic efficiency than the MFC setup without ACPC.

Table 4. Initial and final COD values for MFC-1, MFC-2, and MFC-3.

Characteristics	Initial	Final			
		MFC-1 (2% ACPC and 8% Agar)	MFC-2 (4% ACPC and 6% Agar)	MFC-3 (6% ACPC and 4% Agar)	MFC-A (0% ACPC and 8% Agar)
COD (mg/l)	490.5	167.55	199.34	251.67	260.85
COD Removal Efficiency (%)	-	65.84	59.36	48.69	46.82

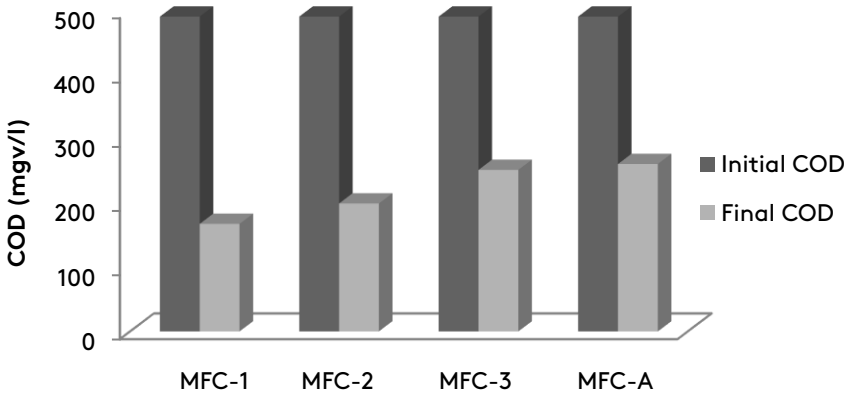

Fig. 6. Comparison of initial and final COD for MFC-1, MFC-2, and MFC-3.

3.5 Coulombic Efficiency (CE)

According to Equation 3, the maximum coulombic efficiency of MFC-1, MFC-2, MFC-3, and MFC-A was 22.84%, 23.4%, 27.96%, and 19.98%, respectively. It was observed that the operation of MFC in a fed-batch mode was advantageous in obtaining a high COD removal rate. Therefore, coulombic efficiencies obtained in these cases were low [45]. MFC-1 had the highest COD removal efficiency; hence, its CE was less compared to MFC-1 and MFC-2. The variation of CE with current density for MFC-1, MFC-2, MFC-3, and MFC-A is shown in Figure 7. It was observed that with the increase in current density, coulombic efficiency also rose. Also, the results showed that the MFC setups with ACPC addition in agar salt bridges had higher coulombic efficiency than the MFC setup without ACPC.

3.6. Power Density

Power density is an important parameter for measuring the efficiency of MFC. The maximum power density obtained by MFC-1, MFC-2, MFC-3, and MFC-A was 61.54 mW/m2, 48.31 mW/m2, 47.53 mW/m2, and 30.22 mW/m2, respectively. MFC-1 achieved the highest power density, which could be attributed to the optimum concentration of ACPC and agar used in the salt bridge, whereas MFC-A achieved the lowest value of power density. It was observed that using ACPC under optimum conditions increased the power density. The variation of power density with time is shown in Figure 8, and the peak values of power density for each MFC setup are given in Table 5. As shown in the present study, conventional agar-based MFCs have low COD removal efficiency that can be enhanced by including activated carbon produced from ACPC in the salt bridge. Although implementing

ACPC in agar salt bridges is novel in this research area, further research in this direction is still required to establish the benefits of its use in preparing the agar salt bridge. The subject area has the potential for further research on the application of hygroscopic oxides, which are capable of improving hydration properties. The graphite electrodes used in the present study are excellent conductors; however, investigations on MFC performance using other electrode types can also be conducted.

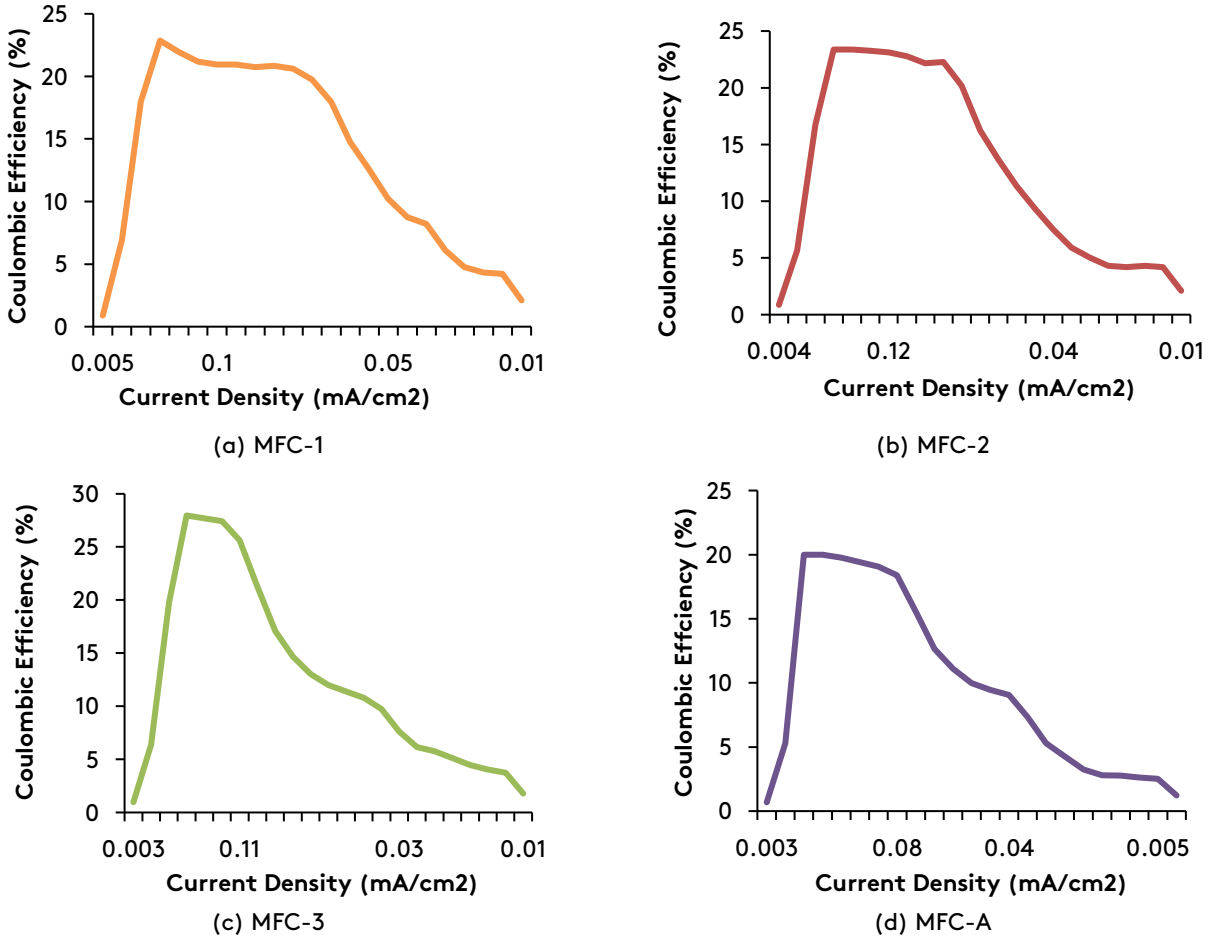

Fig. 7. Variation of Coulombic Efficiency vs Current Density.

Table 5. Peak values of performance parameters for MFC-1, MFC-2, MFC-3, and MFC-A.

Parameter	MFC-1	MFC-2	MFC-3	MFC-A
Open circuit voltage (mV)	421	370	341.05	295
Current (mA)	1.052	0.951	0.938	0.737
COD removal efficiency (%)	65.84	59.36	48.69	46.82
Power density (mW/m^2)	61.54	48.31	47.53	30.22

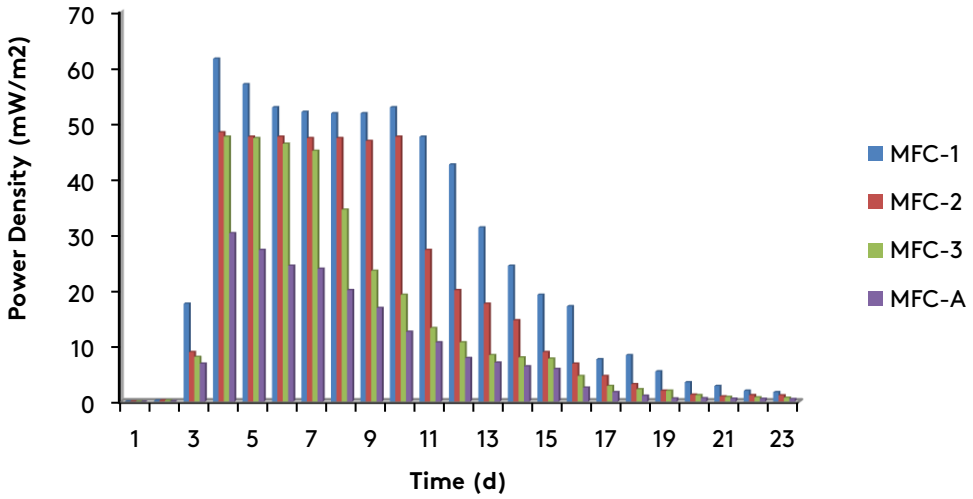

Fig. 8. Variation of Power Density vs time for MFC-1, MFC-2, and MFC-3.

4. Conclusions

The current study examined the impact of employing activated carbon produced from pine cones on the Microbial Fuel Cell's performance. The major indicators used to evaluate the performance of the MFC were COD removal efficiency, current, and open circuit voltage. The peak OCV values measured for MFC-1 (2% ACPC and 8% agar), MFC-2 (4% ACPC and 6% agar), MFC-3 (6% ACPC and 4% agar), and MFC-A (0% ACPC and 8% agar) were 421 mV, 370 mV, 341.05 mV, and 295 mV, respectively. The peak current values obtained for MFC-1, MFC-2, MFC-3, and MFC-A were 1.052 mA, 0.951 mA, 0.938 mA, and 0.737 mA, respectively. The COD removal efficiencies calculated for MFC-1, MFC-2, MFC-3, and MFC-A were 65.84%, 59.36%, 48.69%, and 46.82%, respectively; the maximum power density achieved by MFC-1, MFC-2, MFC-3, and MFC-A was 61.54 mW/m2, 48.31 mW/m2, 47.53 mW/m2 , and 30.22 mW/m2, respectively. The outcome of the study showed that MFC-1 achieved the highest OCV, current, power density, and COD removal efficiency. Effective proton transfer was observed in MFC-1; hence, peak values of the current and OCV were achieved on the fourth day of the experiment. Following this, MFC-1 achieved a steady output until the twelfth day and continued to provide readings up to the twenty-third day of the experiment. Hence, MFC-1, containing 2% ACPC and 8% agar, outperformed the other three MFC setups in terms of performance indicators used in the current study. The outcome of the present study demonstrated the positive impact of ACPC on the agar salt bridge. The study concludes that using ACPC increased the efficacy of proton transfer and helped increase the OCV, power density, and current output of microbial fuel cells. Also, more research is needed to explore the use of ACPC in salt bridges.

Abbreviations

ACPC – Activated carbon produced from pine cones
mV – millivolts
cm – centimeter
mA – milliAmpere
PEM – Proton Exchange Membrane
Mg/l - Milligram per litre
pH – Potential of Hydrogen
CE – Coulombic Efficiency
COD – Chemical Oxygen Demand
OCV – open circuit voltage
mm – millimetres
MFC – Microbial Fuel Cell
ml – millilitres
FAS – Ferrous Ammonium Sulphate
STP – Sewage Treatment Plant
WW – Wastewater

Acknowledgements

The authors acknowledge their colleagues and personnel from the National Institute of Technology, H.P., India, who contributed valuable knowledge and expertise to this study.

Grant Support Details

The present research did not receive any financial support.

Conflict of Interest

The authors declare that there is no conflict of interest regarding the publication of this manuscript. In addition, the authors have completely observed the ethical issues, including plagiarism, informed consent, misconduct, data fabrication and/ or falsification, double publication and/or submission, and redundancy.

References

[1] Dartoomi, H., Khatibi, M., & Ashrafizadeh, S. N. (2022a). Importance of nanochannels shape on blue energy generation in softnanochannels. Electrochimica Acta,431,141175. https://doi.org/10.1016/j.electacta.2022.141175

[2] Dartoomi, H., Khatibi, M., & Ashrafizadeh, S. N. (2022b). Nanofluidic membranes to address the challenges of salinity gradient energy harvesting: roles of nanochannel geometry and bipolar soft layer. Langmuir,38(33),10313-10330. https://doi.org/10.1021/acs.langmuir.2c01790

[3] Karimzadeh, M., Khatibi, M., Ashrafizadeh, S. N., & Mondal, P. K. (2022). Blue energy generation by the temperature-dependent properties in funnel-shaped soft nanochannels. Physical Chemistry Chemical Physics, 24(34), 20303-20317. https:/doi.org/10.1039/D2CP01015A

[4] Khatibi, M., Ashrafizadeh, S. N., & Sadeghi, A. (2021). Augmentation of the reverse electrodialysis power generation in soft nanochannels via tailoring the soft layer properties. Electrochimica Acta, 395, 139221. https://doi.org/10.1016/j.electacta.2021.139221

[5] Khatibi, M., Mojavezi, A., & Pourjafarabadi, E. (2023). Harvesting blue energy: pH-regulated nanochannels inspired by carbon nanostructures. Physics of Fluids, 35(10). https://doi.org/10.1063/5.0170927

[6] Khatibi, M., Dartoomi, H., & Ashrafizadeh, S. N. (2023). Layer-by-layer nanofluidic membranes for promoting blue energy conversion. Langmuir, 39(38), 13717-13734. https://doi.org/10.1021/acs.langmuir.3c01962

[7] Khatibi, M., Sadeghi, A., & Ashrafizadeh, S. N. (2021). Tripling the reverse electrodialysis power generation in conical nanochannels utilizing soft surfaces. Physical Chemistry Chemical Physics, 23(3), 2211-2221. https://doi.org/10.1039/D0CP05974A

[8] Mishra, S., Kumar, R., & Kumar, M. (2023). Use of treated sewage or wastewater as an irrigation water for agricultural purposes-Environmental, health, and economic impacts. Total Environment Research Themes,6,100051. https://doi.org/10.1016/J.TOTERT.2023.100051

[9] Rahimnejad, M., Adhami, A., Darvari, S., Zirepour, A., & Oh, S. E. (2015). Microbial fuel cell as new technol ogy for bioelectricity generation: A review. Alexandria Engineering Journal, 54(3), 745–756. https://doi.org/10.1016/j.aej.2015.03.031

[10] Saravanan, A., Kumar, P. S., Srinivasan, S., Jeevanantham, S., Kamalesh, R., & Karishma, S. (2022). Sustainable strategy on microbial fuel cell to treat the wastewater for the production of green energy. Chemosphere, 290, 133295. https://doi.org/10.1016/J.CHEMOSPHERE.2021.133295

[11] Ye, Y., Ngo, H. H., Guo, W., Chang, S. W., Nguyen, D. D., Liu, Y., Nghiem, L. D., Zhang, X., & Wang, J. (2019). Effect of organic loading rate on the recovery of nutrients and energy in a dual-chamber microbial fuel cell. Bioresource Technology, 281, 367–373. https://doi.org/10.1016/j.biortech.2019.02.108

[12] Shabani, M., Younesi, H., Pontié, M., Rahimpour, A., Rahimnejad, M., & Zinatizadeh, A. A. (2020). A critical review on recent proton exchange membranes applied in microbial fuel cells for renewable energy recovery. Journal of cleaner production, 264, 121446. https://doi.org/10.1016/j.jclepro.2020.121446

[13] Obileke, K. C., Onyeaka, H., Meyer, E. L., & Nwokolo, N. (2021a). Microbial fuel cells, a renewable energy technology for bio-electricity generation: A mini-review. Electrochemistry Communications, 125, 107003. https://doi.org/10.1016/J.ELECOM.2021.107003

[14] Mehri, F., & Rowshanzamir, S. (2019). Electrochemical hydrogenation and desulfurization of thiophenic compounds over MoS2 electrocatalyst using different membrane-electrode assembly. Advances in Environmental Technology, 5(1), 23-33. https://doi.org/10.22104/aet.2019.3647.1178

[15] Prathiba, S., Kumar, P. S., & Vo, D. V. N. (2022). Recent advancements in microbial fuel cells: A review on its electron transfer mechanisms, microbial community, types of substrates and design for bio-electrochemical treatment. Chemosphere, 286, 131856. https://doi.org/10.1016/J.CHEMOSPHERE.2021.131856

[16] Neethu, B., Bhowmick, G. D., & Ghangrekar, M. M. (2019). A novel proton exchange membrane developed from clay and activated carbon derived from coconut shell for application in microbial fuel cell. Biochemical Engineering Journal, 148, 170-177. https://doi.org/10.1016/j.bej.2019.05.011

[17] Nawaz, A., ul Haq, I., Qaisar, K., Gunes, B., Raja, S. I., Mohyuddin, K., & Amin, H. (2022). Microbial fuel cells: Insight into simultaneous wastewater treatment and bioelectricity generation. Process Safety and Environmental Protection, 161, 357–373. https://doi.org/10.1016/J.PSEP.2022.03.039

[18] Singh, K., & Dharmendra. (2020). Optimization and performance evaluation of microbial fuel cell by varying agar concentration using different salts in salt bridge medium. Archives of Materials Science and Engineering, 101(2), 79–84. https://doi.org/10.5604/01.3001.0014.1193

[19] Hu, X., Tan, X., Shi, X., Liu, W., & Ouyang, T. (2023). An integrated assessment of microfluidic microbial fuel cell subjected to vibration excitation. Applied Energy, 336, 120852. https://doi.org/10.1016/j.apenergy.2023.120852

[20] Zhao, K., Shu, Y., Li, F., & Peng, G. (2023). Bimetallic catalysts as electrocatalytic cathode materials for the oxygen reduction reaction in microbial fuel cell: A review. Green Energy & Environment, 8(4), 1043-1070. https://doi.org/10.1016/j.gee.2022.10.007

[21] Arun, J., SundarRajan, P., Pavithra, K. G., Priyadharsini, P., Shyam, S., Goutham, R., ... & Pugazhendhi, A. (2024). New insights into microbial electrolysis cells (MEC) and microbial fuel cells (MFC) for simultaneous wastewater treatment and green fuel (hydrogen) generation. Fuel, 355, 129530. https://doi.org/10.1016/j.fuel.2023.129530

[22] ter Heijne, A., Hamelers, H. V. M., Saakes, M., & Buisman, C. J. N. (2008). Performance of non-porous graphite and titanium-based anodes in microbial fuel cells. Electrochimica Acta, 53(18), 5697–5703. https://doi.org/10.1016/j.electacta.2008.03.032

[23] Asensio, Y., Montes, I. B., Fernandez-Marchante, C. M., Lobato, J., Cañizares, P., & Rodrigo, M. A. (2017). Selection of cheap electrodes for two-compartment microbial fuel cells. Journal of Electroanalytical Chemistry, 785, 235-240. https://doi.org/10.1016/j.jelechem.2016.12.045

[24] Yaqoob, A. A., Ibrahim, M. N. M., & Rodríguez-Couto, S. (2020). Development and modification of materials to build cost-effective anodes for microbial fuel cells (MFCs): An overview. Biochemical Engineering Journal, 164, 107779. https://doi.org/10.1016/J.BEJ.2020.107779

[25] Zhang, F., Cheng, S., Pant, D., Bogaert, G. Van, & Logan, B. E. (2009). Power generation using an activated carbon and metal mesh cathode in a microbial fuel cell. Electrochemistry Communications, 11(11), 2177–2179. https://doi.org/10.1016/J.ELECOM.2009.09.024

[26] Arena, N., Lee, J., & Clift, R. (2016). Life Cycle Assessment of activated carbon production from coconut shells. Journal of Cleaner Production, 125, 68-77. https://doi.org/10.1016/j.jclepro.2016.03.073

[27] Gajda, I., Greenman, J., & Ieropoulos, I. (2020). Microbial Fuel Cell stack performance enhancement through carbon veil anode modification with activated carbon powder. Applied Energy, 262, 114475. https://doi.org/10.1016/J.APENERGY.2019.114475

[28] Matsena, M. T., Mabuse, M., Tichapondwa, S. M., & Chirwa, E. M. N. (2021). Improved performance and cost efficiency by surface area optimization of granular activated carbon in air-cathode microbial fuel cell. Chemosphere, 281, 130941. https://doi.org/10.1016/J.CHEMOSPHERE.2021.130941

[29] Wei, B., Tokash, J. C., Chen, G., Hickner, M. A., & Logan, B. E. (2012). Development and evaluation of carbon and binder loading in low-cost activated carbon cathodes for air-cathode microbial fuel cells. RSC Advances, 2(33), 12751–12758. https://doi.org/10.1039/C2RA21572A

[30] Chien, H. C., Tsai, L. D., Lai, C. M., Lin, J. N., Zhu, C. Y., & Chang, F. C. (2013). Characteristics of high-water-uptake activated carbon/Nafion hybrid membranes for proton exchange membrane fuel cells. Journal of Power Sources, 226, 87–93. https://doi.org/10.1016/J.JPOWSOUR.2012.10.017

[31] Tsai, L. D., Chien, H. C., Wang, C. H., Lai, C. M., Lin, J. N., Zhu, C. Y., & Chang, F. C. (2013). Poly(ethylene glycol) modified activated carbon for high performance proton exchange membrane fuel cells. International Journal of Hydrogen Energy, 38(26), 11331–11339. https://doi.org/10.1016/J.IJHYDENE.2013.06.054

[32] Kammoun, M., Lundquist, L., & Ardebili, H. (2015). High proton conductivity membrane with coconut shell activated carbon. Ionics, 21(6), 1665–1674. https://doi.org/10.1007/s11581-014-1311-0

[33] Ayrilmis, N., Buyuksari, U., & Dundar, T. (2010). Waste pine cones as a source of reinforcing fillers for thermoplastic composites. Journal of Applied Polymer Science, 117(4), 2324–2330. https://doi.org/10.1002/APP.32076

[34] Duman, G., Onal, Y., Okutucu, C., Onenc, S., & Yanik, J. (2009). Production of Activated Carbon from Pine Cone and Evaluation of Its Physical, Chemical, and Adsorption Properties. Energy and Fuels, 23(4), 2197–2204. https://doi.org/10.1021/EF800510M

[35] Uddin, S. S., Prodhan, M. M. H., & Nurnabi, M. (2024). Studies on agar salt bridge based dual chamber microbial fuel cells using sludge and dustbin waste. Biomass Conversion and Biorefinery, 1-9. https://doi.org/10.1007/s13399-024-05718-8

[36] Chen, X., Fu, X., Huang, L., Xu, J., & Gao, X. (2021). Agar oligosaccharides: A review of preparation, structures, bioactivities and application. Carbohydrate Polymers, 265, 118076. https://doi.org/10.1016/J.CARBPOL.2021.118076

[37] Aguiar, J. B. (1999). Durability of polymeric pipes in contact with domestic products. Construction and Building Materials, 13(3), 155–157. https://doi.org/10.1016/S0950-0618(98)00035-X

[38] Heidari Farsani, M., Jalilzadeh Yengejeh, R., Hajiseyed Mirzahosseini, A., Monavari, M., Hassani, A. H., & Mengelizadeh, N. (2021). Study of the performance of bench-scale electro-membranes bioreactor in leachate treatment. Advances in Environmental Technology, 7(3), 209-220. https://doi.org/10.22104/aet.2022.5266.1426

[39] Ghasemi, M., Shahgaldi, S., Ismail, M., Yaakob, Z., & Daud, W. R. W. (2012). New generation of carbon nanocomposite proton exchange membranes in microbial fuel cell systems. Chemical Engineering Journal, 184, 82-89. https://doi.org/10.1016/j.cej.2012.01.001

[40] Chen, W., Liu, Z., Li, Y., Xing, X., Liao, Q., & Zhu, X. (2021). Improved electricity generation, coulombic efficiency and microbial community structure of microbial fuel cells using sodium citrate as an effective additive. Journal of Power Sources, 482, 228947. https://doi.org/10.1016/J.JPOWSOUR.2020.228947

[41] Qazani, M. R. C., Ghasemi, M., & Asadi, H. (2024). Optimizing microbial fuel cells with multiple-objectives PSO and type-2 fuzzy neural networks. Fuel, 372, 132090. https://doi.org/10.1016/j.fuel.2024.132090

[42] Huang, L., Regan, J. M., & Quan, X. (2011). Electron transfer mechanisms, new applications, and performance of biocathode

microbial fuel cells. Bioresource Technology, 102(1), 316–323. https://doi.org/10.1016/J.BIORTECH.2010.06.096

[43] Hernández-Flores, G., Andrio, A., Compañ, V., Solorza-Feria, O., & Poggi-Varaldo, H. M. (2019). Synthesis and characterization of organic agar-based membranes for microbial fuel cells. Journal of Power Sources, 435, 226772. https://doi.org/10.1016/J.JPOWSOUR.2019.226772

[44] Yi, H., Nevin, K. P., Kim, B. C., Franks, A. E., Klimes, A., Tender, L. M., & Lovley, D. R. (2009). Selection of a variant of Geobacter sulfurreducens with enhanced capacity for current production in microbial fuel cells. Biosensors and Bioelectronics, 24(12), 3498–3503. https://doi.org/10.1016/J.BIOS.2009.05.004

[45] Obileke, K. C., Onyeaka, H., Meyer, E. L., & Nwokolo, N. (2021b). Microbial fuel cells, a renewable energy technology for bio-electricity generation: A mini-review. Electrochemistry Communications, 125, 107003. https://doi.org/10.1016/J.ELECOM.2021.107003

How to cite this paper:

Saini, A. & Shankar, V. (2025). Investigating Microbial Fuel Cell Performance by Developing Salt Bridge from Agar and Activated Carbon Derived from Pine Cones. Advances in Environmental Technology, 11(2), 116-129. DOI: 10.22104/AET.2024.7008.1923